

Substrate doping effects on Raman spectrum of epitaxial graphene on SiC

R. Yang, Q. S. Huang, X. L. Chen, G. Y. Zhang,^{a)} and H.-J. Gao
Nanoscale Physics and Device Laboratory, Institute of Physics, Chinese Academy of Sciences, Beijing 100190, China

(Received 26 November 2008; accepted 5 December 2009; published online 2 February 2010)

In this paper, we reported a Raman scattering study of epitaxial graphene on different doped 6H-SiC (0001) substrates and investigated the substrate induced charge-transfer doping to the epitaxial graphene. We found that the charge carrier type and concentration of epitaxial graphene can be altered by SiC substrates with different doping level and doping type. This effect is comparable to that obtained by electrochemical doping. As Raman scattering is very sensitive to the doping level, the charge carrier concentration of epitaxial graphene can be estimated by the Raman G-peak shift. Our results are fundamental and may have implications for future epitaxial-graphene-based micro/nanoelectronic devices. © 2010 American Institute of Physics. [doi:10.1063/1.3283922]

I. INTRODUCTION

Graphene and graphene multilayer grown epitaxially on the single-crystalline silicon carbide (SiC) by Si depletion^{1,2} have attracted much attention recently due to their unique properties. The epitaxial growth technique is one strategy for the wafer-scale production of graphene,³ as the other methods show difficulties to get large scale and uniform samples up to now. As the epitaxial graphene on SiC shows great potential for future electronic devices, it is very fundamental to control the charge carrier doping. Substitution doping for epitaxial graphene is not available so far and an alternative way to control its charge carrier is to use either external gating^{4,5} or internal doping. Recently, both experimental and theoretical studies have revealed the charge transfer doping for epitaxial graphene by adsorbing atoms or molecules on its surface.^{6,7} However, the adsorption is unstable and the doping also includes the contribution from the SiC substrate. Thus, it is very important to understand the charge transfer between SiC and graphene in order to control the charge carrier doping.

Raman scattering has been proved to be a powerful tool for investigating the electron-phonon interaction of the carbon-based materials.⁸ The G and the 2D bands are particularly interesting for studying the effect of strain or doping-induced charge transfer.^{8–11} Various Raman studies of epitaxial graphene on the SiC have been done recently^{12–19} with focus on the layer numbers and the in-plane strain. However, there is still insufficient data addressing the substrate doping effect. In this work, we have prepared epitaxial graphene on different doped 6H-SiC (0001) substrates and studied the substrate doping effect by Raman spectroscopy.

II. EXPERIMENTAL DETAILS

The epitaxial graphene was prepared first on different N-doped 6H-SiC (0001) substrates provided by Tanke-Blue Industries, Beijing, China, one was lightly doped (type-I) and another heavily doped (type-II). Table I lists several electri-

cal parameters of the two substrates measured by BIO-RAD Microscience Division HL5200 Hall system at the room temperature. Prior to growth, the 6H-SiC (0001) substrates were calcined in hydrogen atmosphere first at 1600 °C for 10 min to remove polishing damages. During the growth, the substrate was loaded into a hot-wall chemical vapor deposition reactor. The growth environment was pumped to a base pressure of 2×10^{-5} Pa under an Ar flow protection. After a preliminary heating at 1050 °C for 30 min to remove the native oxide, the substrate was then heated at 1350 °C for 5–10 min then cooled down to room temperature.³ The sample surface topography was imaged by atomic force microscopy (AFM) (Nanoscope Multimode SPM from Veeco) and the average thickness of the as-grown graphene was checked by x-ray photoelectron spectroscopy (XPS) (ESCALAB-5 from VG). Raman spectra were collected by a JY-T64000 high-resolution Raman spectrometer using a He-Ne laser ($\lambda=632.8$ nm, power=8.6 mW).

III. RESULTS AND DISCUSSIONS

AFM image of a polished on-axis N-doped 6H-SiC (0001) substrate is shown in Fig. 1(a) in which scratches can be clearly seen. After calcining in hydrogen at 1600 °C for 10 min, scratches disappeared and regular steps formed on the surface [Fig. 1(b)]. Epitaxial graphene was grown at 1350 °C and steplike features indicating its discrete and layered structure [Figs. 1(c) and 1(d)]. Scanning tunneling microscope image of as grown graphene [inset of Fig. 1(d)] shows clear moiré pattern resulted by the mismatch between the monolayer epitaxial graphene and the SiC substrate.

Figure 2(a) plots typical Raman spectra of epitaxial graphene grown on the type-I substrate with different layers. In comparison, Raman spectrum from bare SiC and highly oriented pyrolytic graphite (HOPG) are also included. The average layer number of the epitaxial graphene [marked in Fig. 2(a)] was estimated from the attenuation of the substrate Raman signal²⁰ and was also confirmed by XPS. Raman spectra of sp^2 carbon have several fingerprint features, including G-line, D-line, and 2D-line. The G-line,^{14,17} assigned to an E_{2g} phonon mode at the center of the Brillouin zone, is

^{a)}Author to whom correspondence should be addressed. Electronic mail: gyzhang@aphy.iphy.ac.cn.

TABLE I. Room temperature Hall measurement parameter of bared 6H-SiC (0001) substrate.

6H-SiC (0001)	Resistivity (Ω cm)	Mobility ($\text{cm}^2/\text{V s}$)	Carrier concentration (n) (cm^{-3})	Hall-coefficient (cm^3/c)
I (lightly N-doped)	1.66×10^6	73	3.925×10^{15}	1575.56
II (heavily N-doped)	0.043589	155	9.301×10^{17}	-6.76

an indication of sp^2 -carbon components. The D-line,^{14,21} caused by a defect-assisted one-phonon double resonance effect, exhibits two remarkable features: it shifts to higher frequencies with increasing incident laser excitation energies and its relative signal strength (compared to the G line) depends strongly on the amount of disorder or the size of the crystal. The related 2D-line overtone, a reflection of a two-phonon double resonance effect,^{17,22} is very sensitive to the electronic structure and the stacking order along the c -axis. From Figs. 2(b), 2(d), and 2(e), we can clearly see that the graphene G peak is redshifted with increasing layer numbers, while the peak full width at half maximum (FWHM) does not change. The graphene G peak is also blueshifted compared to that of HOPG or cleaved graphene but not as much as that reported before.^{12,13} The small shoulder appeared around 1620 cm^{-1} is caused by the small crystalline size of epitaxial graphene.²³ We conclude that epitaxial graphene composes of many graphene crystalline domains with the same orientation. The graphene crystalline size, which depends on the growth temperature, the growth duration, and the quality of the substrate, can also be deduced from the ratio $I(\text{D})/I(\text{G})$ by the Tuinstra-Koenig relationship.^{22,24} The graphene 2D peak is broadened and blueshifted with increasing layer numbers, as shown in Figs. 2(c)–2(e). The overall 2D peak for epitaxial graphene on SiC is also blueshifted as compared to the cleaved graphene on SiO_2 . Moreover, the 2D-peak shape, which was only be fitted by a single

Lorentzian, shows no clear asymmetry, nor a shoulder, even when the stacked layer numbers exceed ten. The stacking order of our epitaxial graphene prepared in low-vacuum may not follow the A-B stacking style,^{15,25,26} as the stacking order could be misoriented in some growth condition even on Si-face.^{3,27,28}

The Raman spectra of epitaxial graphene grown on the two different N-doped 6H-SiC (0001) substrates are clearly different [Fig. 3(a)]. Epitaxial graphene grown on type-II substrate has much higher G- and 2D-band frequencies at 1593.4 and 2674.8 cm^{-1} , respectively, compared to 1588.5 and 2665.8 cm^{-1} for epitaxial graphene on type-I substrate. As the epitaxial graphene grows thicker on type-II substrate, all three Raman peaks, D, G, and 2D show lower frequencies [as shown in Fig. 3(b)]. This redshift behavior may be resulted from the screening effect as the charge carrier doping can be screened by the lower layers of the thick graphene. Notice that the 2D-peak shifts for graphene on type-II substrate are contrary to those on type-I substrate, and the G-peak shifts for graphene on type-II substrate are bigger than that for type-I substrate, as shown in Figs. 3(c) and 3(d).

As we know, several groups have already reported that the G- and the 2D-peak shifts for graphene are influenced by the strain effect^{12,18,19} and charge-transfer doping effect.¹¹ Based on their first-principle calculations, the uniaxial strain, which breaks the symmetry of sublattice and affects the electronic properties of graphene, leads to the redshifts of the 2D and the G bands as well as the G-peak splitting.¹⁹ In comparison, the biaxial strain does not move the relative positions of the Dirac cones, so the biaxial strain only leads to the blueshift (compressive strain) or the redshift (tensile strain) of the G and the 2D peaks.^{12,19}

Ferrari *et al.*^{9,29} have also studied the doping effect on mechanically exfoliated graphene by exploiting the time-dependent perturbation theory. The charge-transfer doping effect, which influences the Fermi surface of graphene and moves the Kohn anomaly away from $q=0$, is an effect of nonadiabatic Kohn anomaly.³⁰ Doping can result in a stiffening of the $E_{2g}\Gamma$ phonon (G line), and the G peak can be blueshifted as the charge carrier concentration goes high. The G-peak shifts can be described as: $[h/(2\pi)]\Delta\omega(G) = \alpha' P \int_{-\infty}^{\infty} \{ [f(\varepsilon - \varepsilon_F) - f(\varepsilon)] \varepsilon^2 \sin(\varepsilon) \} / \{ \varepsilon^2 - [(h/2\pi)w_0] \} (d\varepsilon)$, where $\alpha=4.39 \times 10^{-3}$, P is the principal part, and f is the Fermi-Dirac distribution at T . Here, time-dependent perturbation theory was only fitted for phonons at Γ point. For the phonons between K and M point, the nonadiabatic effects are negligible due to the double resonance. As a result, the effect of charge-transfer doping in this case can still be described by a standard adiabatic phonon calculation¹⁰ and the position of the 2D peak shows a redshift for an increasing electron concentration.

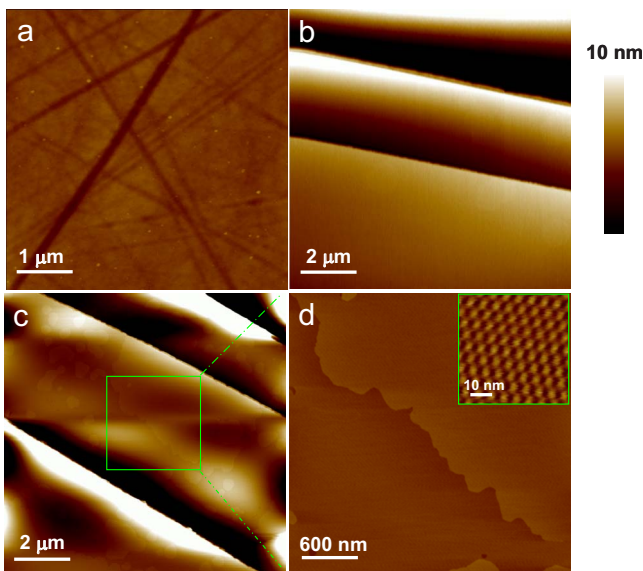


FIG. 1. (Color online) AFM images of the polished 6H-SiC (0001) substrate (a) before and (b) after H_2 anneal; [(c) and (d)] zoom in image for marked area in (c), show the initial growth stage of epitaxial graphene prepared in our experiment. The inset of (d) shows the STM image of the formed moiré pattern scanned by Pt/Ir tip in air at $V=20 \text{ mV}$, $I=1 \text{ nA}$.

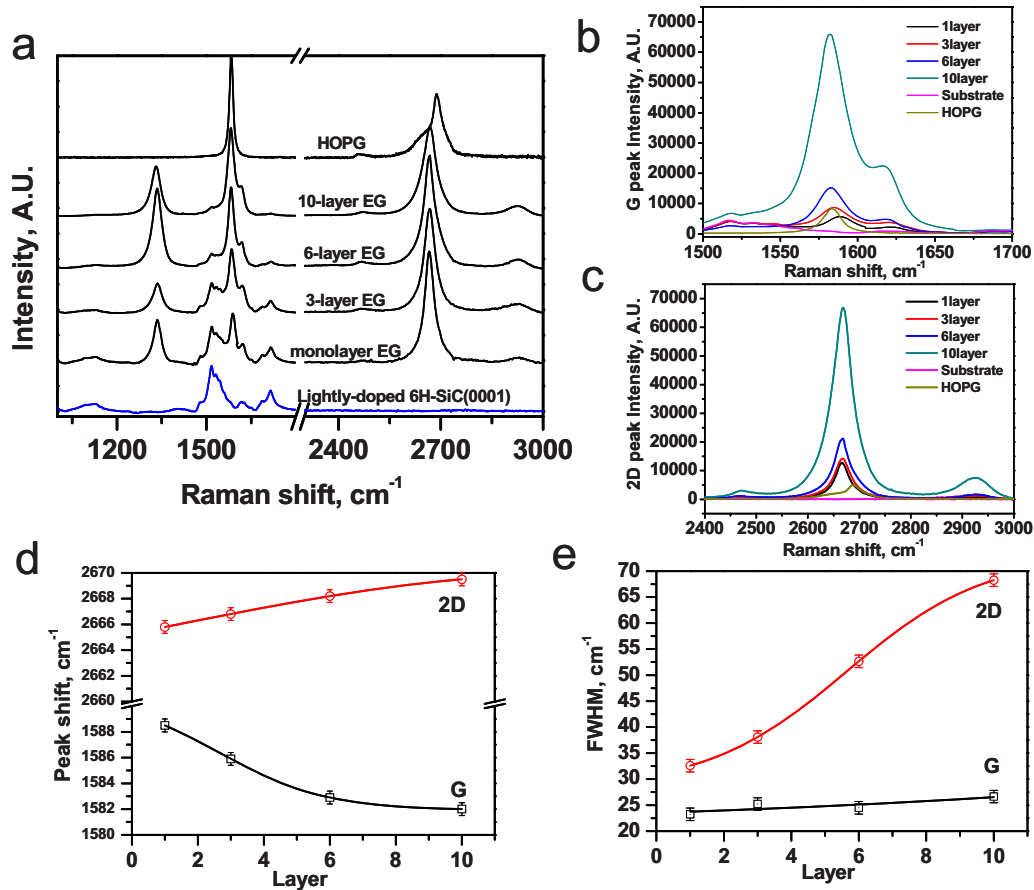


FIG. 2. (Color online) (a) Typical Raman spectra of a monolayer, a triple-layer, a six-layer and a ten-layer epitaxial graphene on the lightly N-doped 6H-SiC (0001), together with the reference spectra on the bare 6H-SiC (0001) substrate, as well as HOPG; (b) and (c) show the Raman peak positions for the G-band and the 2D-band with varying numbers of the epitaxial graphene layers, respectively; (d) and (e), respectively, illustrates the variation fits of the G-band and the 2D-band frequency as well as FWHM against the number of the epitaxial graphene layers.

The two different N-doped 6H-SiC (0001) substrates we used for growth were fine-polished and have smooth surfaces after calcinations in H₂ [see AFM image Fig. 1(b)]. The doping level does not change the crystal lattice structure of SiC. The strain is most likely to be the biaxial strain induced by the lattice mismatch between the graphene and the substrate. Besides, the cooling process can also influence the biaxial strain. As for our samples, the growth conditions are the same, so the difference of the biaxial strain induced by the cooling process can also be excluded. Hence, the unusual distinction of the Raman G-peak of epitaxial graphene on the two types of substrates may originate from the charge-transfer doping. In the case of electron transfer to graphene through the heavily N-doped 6H-SiC (0001) substrate, the graphene G-peak is blueshifted. In comparison, the Raman G-peak of epitaxial graphene on lightly N-doped substrate is similar to that of the mechanically exfoliated graphene, as the charge transfer effect is small [Figs. 3(c) and 3(d)].⁸ However, the 2D peak of the epitaxial graphene on the heavily N-doped substrate shows significant blueshift to that on the lightly N-doped substrate, which is inconsistent with the calculated results.^{9,11} This distinction might be caused by the strain inhomogeneity as reported by Robinson *et al.*³¹

Doping induced charge transfer can also make significant decrease in the G-peak linewidth [FWHM(G)] for epitaxial graphene.⁹ The G phonon ($q_G \approx 0$) is sensitive to the

carrier density according to the Pauli exclusion principle.^{9,28} In comparison, the decay of the D-phonon dispersion with large wave vector q_D is unaffected in the case of low doping. Thus the 2D linewidth keep constant except that the Fermi level shift induced by charge-transfer is close to the exciting laser energy.^{11,32} In our results, the FWHM of the 2D line stays constant at 33 ± 0.5 cm⁻¹ and does show no doping dependence. The FWHM of the G-line of epitaxial graphene on the type-I substrate is 24 cm⁻¹ compared to 31 cm⁻¹ for epitaxial graphene on the type-II substrate. Moreover, the relative intensity $I(2D)/I(G)$ also shows a large variation from different doping level: $I(2D)/I(G)$ is ~ 2.2 at low doping and is ~ 1.7 at high doping.

Based on the above discussion we conclude that the observation of different Raman scattering for epitaxial graphene grown on the two different N-doped substrates is caused by the charge transfer between the SiC substrates and the graphene. The G-peak shift is an indication of how much charge is transferred to epitaxial graphene. If we assume a charge neutrality point and filter the biaxial strain effect, we can estimate the carrier density of epitaxial graphene by using the G-peak shift from the time-dependent perturbation theory.⁹

To further explore the substrate charge-transfer effect, we also grew graphene on both N-doped and P-doped 6H-

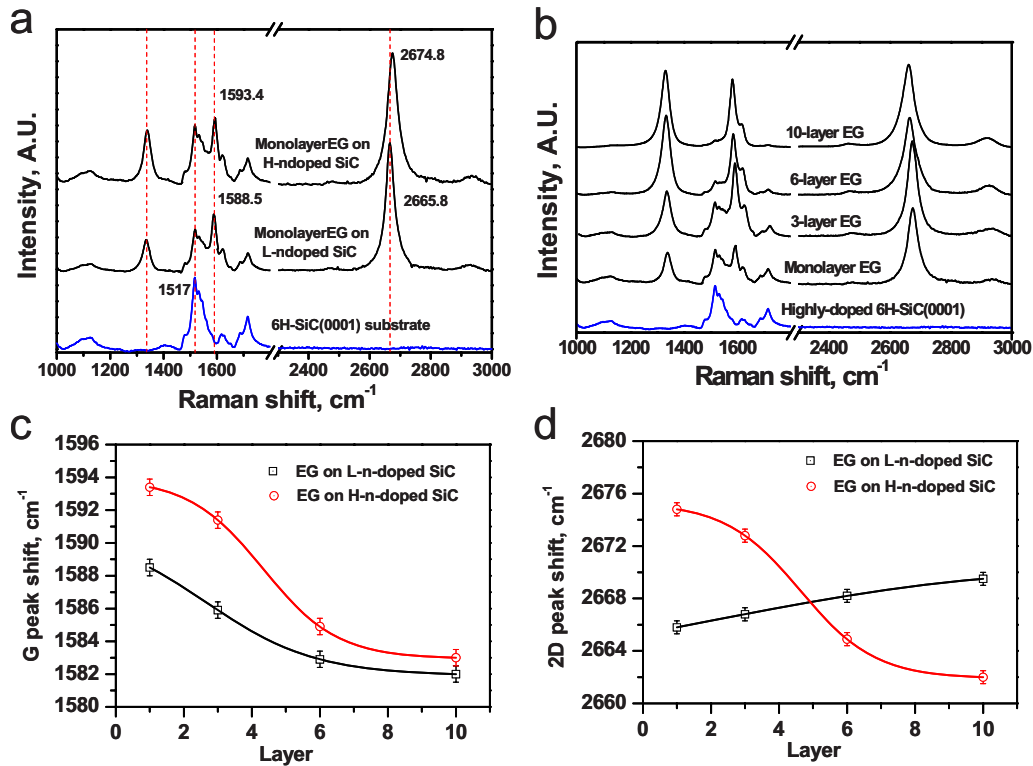


FIG. 3. (Color online) (a) Raman spectra of monolayer epitaxial graphene grown on the different N-doped 6H-SiC (0001) substrates, together with the reference spectra on the bare 6H-SiC (0001) substrate; (b) Raman spectra of a monolayer, triple-layer, six-layer and ten-layer epitaxial graphene grown on the heavily N-doped 6H-SiC (0001); (c) and (d), respectively, illustrates the variation fits of the G-band and the 2D-band frequency of epitaxial graphene on the two differently N-doped substrates against the number of layers.

SiC (0001) substrates with different doping level. The graphene G peaks are presented in Fig. 4(a). Similar trends were found in the Raman G-peak shifts with different layer

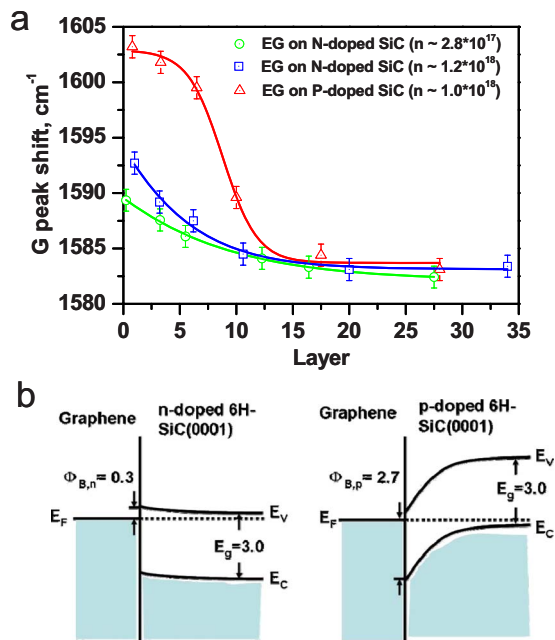


FIG. 4. (Color online) (a) Fits of the Raman G-peak shifts of epitaxial graphene grown on different-doped 6H-SiC (0001) substrates with different layer numbers: on medium N-doped substrate (\circ), on high N-doped substrate (\square) and on highly P-doped substrate (\triangle). (b) Schematic illustration of the charge transfer between epitaxial graphene and 6H-SiC (0001) system.

numbers. We note that, under the same substrate charge carrier concentration, the G peaks of epitaxial graphene grown on the P-doped substrate [Fig. 4(a) (\triangle)] shift more than on the N-doped substrate [Fig. 4(a) (\square)]. This might be caused by the different Schottky barriers between the epitaxial graphene and 6H-SiC substrate with different doping type,^{33–35} as shown in Fig. 4(b). With the same Fermi level, the charge transfer from P-doped substrate is higher than that from N-doped substrate. Hence, the doping type of 6H-SiC may also influence the substrate doping effect.

IV. CONCLUSION

In summary, we carried out Raman spectroscopic studies for epitaxial graphene grown on the differently doped 6H-SiC (0001) substrate. The present study establishes that the Raman spectrum of epitaxial graphene is sensitive to the substrate charge-transfer doping, and the charge carrier type and concentration of epitaxial graphene can be altered by different substrates. These effects are comparable to those obtained by electrochemical doping. The use of differently doped SiC substrates to grow epitaxial graphene provides a simple way to dope graphene, thus we can choose proper substrates for graphene growth to meet the requirement of various devices making.

ACKNOWLEDGMENTS

This work was supported by the IOP starting funding for young scientists, CAS starting funding for “National 100 excellent Ph.D. thesis award” winners, and National 973

projects of China (Grant No. 2010CB934202), Chinese Academy of Sciences (CAS), and National Natural Science Foundation of China (Grant No. 50972162).

- ¹W. A. Deheer, C. Berger, X. S. Wu, P. N. First, E. H. Conrad, X. B. Li, T. B. Li, M. Sprinkle, J. Hass, M. L. Sadowski, M. Potemski, and G. Martinez, *Solid State Commun.* **143**, 92 (2007).
- ²J. Hass, W. A. de Heer, and E. H. Conrad, *J. Phys.: Condens. Matter* **20**, 323202 (2008).
- ³K. V. Emtsev, A. Bostwick, K. Horn, J. Jobst, G. L. Kellogg, L. Ley, J. L. McChesney, T. Ohta, S. A. Reshanov, J. Röhrl, E. Rotenberg, A. K. Schmid, D. Waldmann, H. B. Weber, and T. Seyller, *Nature Mater.* **8**, 203 (2009).
- ⁴J. Kedzierski, P. L. Hsu, P. Healey, P. W. Wyatt, C. L. Keast, M. Sprinkle, C. Berger, and W. A. de Heer, *IEEE Trans. Electron Devices* **55**, 2078 (2008).
- ⁵Y. Q. Wu, P. D. Ye, M. A. Capano, Y. Xuan, Y. Sui, M. Qi, J. A. Cooper, T. Shen, D. Pandey, G. Prakash, and R. Reifengerger, *Appl. Phys. Lett.* **92**, 092102 (2008).
- ⁶I. Gierz, C. Riedl, U. Starke, C. R. Ast, and K. Kern, *Nano Lett.* **8**, 4603 (2008).
- ⁷W. Chen, S. Chen, D. C. Qui, X. Y. Gao, and A. T. S. Wee, *J. Am. Chem. Soc.* **129**, 10418 (2007).
- ⁸A. C. Ferrari, *Solid State Commun.* **143**, 47 (2007).
- ⁹S. Pisana, M. Lazzeri, C. Casiraghi, K. S. Novoselov, A. K. Geim, A. C. Ferrari, and F. Mauri, *Nature Mater.* **6**, 198 (2007).
- ¹⁰C. Casiraghi, S. Pisana, K. S. Novoselov, A. K. Geim, and A. C. Ferrari, *Appl. Phys. Lett.* **91**, 233108 (2007).
- ¹¹A. Das, S. Pisana, B. Chakraborty, S. Piscanec, S. K. Saha, U. V. Waghmare, K. S. Novoselov, H. R. Krishnamurthy, A. K. Geim, A. C. Ferrari, and A. K. Sood, *Nat. Nanotechnol.* **3**, 210 (2008).
- ¹²Z. H. Ni, W. Chen, X. F. Fan, J. L. Kuo, T. Yu, A. T. S. Wee, and Z. X. Shen, *Phys. Rev. B* **77**, 115416 (2008).
- ¹³J. Röhrl, M. Hundhausen, K. V. Emtsev, Th. Seyller, R. Graupner, and L. Ley, *Appl. Phys. Lett.* **92**, 201918 (2008).
- ¹⁴A. C. Ferrari, J. C. Meyer, V. Scardaci, C. Casiraghi, M. Lazzeri, F. Mauri, S. Piscanec, D. Jiang, K. S. Novoselov, S. Roth, and A. K. Geim, *Phys. Rev. Lett.* **97**, 187401 (2006).
- ¹⁵C. Faugeras, A. Nerrière, M. Potemski, A. Mahmood, E. Dujardin, C. Berger, and W. A. de Heer, *Appl. Phys. Lett.* **92**, 011914 (2008).
- ¹⁶S. Shivaraman, M. V. S. Chandrashekar, and M. G. Spencer, *J. Electron. Mater.* **38**, 725 (2009).
- ¹⁷D. S. Lee, C. Riedl, B. Krau, K. von Klitzing, U. Starke, and J. H. Smet, *Nano Lett.* **8**, 4320 (2008).
- ¹⁸Z. H. Ni, T. Yu, Y. H. Lu, Y. Y. Wang, Y. P. Feng, and Z. X. Shen, *ACS Nano* **2**, 2301 (2008).
- ¹⁹T. M. G. Mohiuddin, A. Lombardo, R. R. Nair, A. Bonetti, G. Savini, R. Jalil, N. Bonini, D. M. Basko, C. Galiotis, N. Marzari, K. S. Novoselov, A. K. Geim, and A. C. Ferrari, *Phys. Rev. B* **79**, 205433 (2009).
- ²⁰S. Shivaraman, M. V. S. Chandrashekar, J. J. Boeckl, M. G. Spencer, and J. Electro. Mater. Chem. **38**, 725 (2009).
- ²¹F. Tuinstra and J. Koenig, *J. Chem. Phys.* **53**, 1126 (1970).
- ²²A. C. Ferrari and J. Robertson, *Phys. Rev. B* **61**, 14095 (2000).
- ²³M. A. Pimenta, G. Dresselhaus, M. S. Dresselhaus, L. G. Cancado, A. Jorio, and R. Saito, *Phys. Chem. Chem. Phys.* **9**, 1276 (2007).
- ²⁴R. Vidano and D. B. Fischbach, *J. Am. Ceram. Soc.* **61**, 13 (1978).
- ²⁵J. Hass, R. Feng, J. E. Millán-Otoya, X. Li, M. Sprinkle, P. N. First, W. A. de Heer, E. H. Conrad, and C. Berger, *Phys. Rev. B* **75**, 214109 (2007).
- ²⁶A. Mattausch and O. Pankratov, *Phys. Rev. Lett.* **99**, 076802 (2007).
- ²⁷P. Sutter, *Nature Mater.* **8**, 171 (2009).
- ²⁸T. Ohta, A. Bostwick, J. L. McChesney, T. Seyller, K. Horn, and E. Rotenberg, *Phys. Rev. Lett.* **98**, 206802 (2007).
- ²⁹J. Yan, Y. Zhang, P. Kim, and A. Pinczuk, *Phys. Rev. Lett.* **98**, 166802 (2007).
- ³⁰M. Lazzeri and F. Mauri, *Phys. Rev. Lett.* **97**, 266407 (2006).
- ³¹J. A. Robinson, C. P. Puls, N. E. Staley, J. P. Stitt, M. A. Fanton, K. V. Emtsev, T. Seyller, and Y. Liu, *Nano Lett.* **9**, 946 (2009).
- ³²S. Piscanec, M. Lazzeri, F. Mauri, A. C. Ferrari, and J. Robertson, *Phys. Rev. Lett.* **93**, 185503 (2004).
- ³³S. J. Sque, R. Jones, and P. R. Briddon, *Phys. Status Solidi A* **204**, 3708 (2008).
- ³⁴S. A. Reshanov, K. Emtsev, F. Speck, K. Y. Gao, T. Seyller, G. Pensl, and L. Ley, *Phys. Status Solidi B* **245**, 1369 (2008).
- ³⁵T. Seyller, K. Emtsev, F. Speck, K. Y. Gao, and L. Ley, *Appl. Phys. Lett.* **88**, 242103 (2006).